Materials Research Proceedings 33 (2023) 269-276 https://doi.org/10.21741/9781644902677-39

Simulations of vertical sloshing in a partially filled rectangular tank subjected to time-periodic excitation

Daniele Rossi [1,a *]

[1]Dipartimento di Ingegneria Meccanica e Aerospaziale, Sapienza Università di Roma, via Eudossiana 18, Rome, 00184, Italy

[a]daniele.rossi@uniroma1.it

Keywords: Sloshing, Multiphase Flows, VOF Solver, Energy Dissipation

Abstract. An in-house Navier-Stokes multiphase VOF (Volume-Of-Fluid) solver is used to study sloshing phenomena in a partially filled rectangular tank subjected to vertical sinusoidal excitation. The flow dynamics is found to be significantly affected by vertical acceleration and forcing frequency. Specifically, when the acceleration is strong and the excitation frequency is low, the flow exhibits a more chaotic and three-dimensional nature. Consequently, certain properties such as the energy dissipation and the mixing efficiency of the system are poorly predicted by two-dimensional simulations in that range of parameters, making more expensive three-dimensional simulations necessary. The time history of the sloshing force and instantaneous flow visualizations are used to analyze the effects of liquid impacting on the walls on energy exchanges between the fluid and the tank. Finally, the evolution of mixing efficiency and its influence on the energy losses are discussed.

Introduction

The term sloshing generally refers to motion of free liquid inside a partially filled container, resulting from any form of disturbance or imparted excitation. Depending on the type of disturbance and container shape, the liquid free surface can experience various types of motion. Vertical sloshing is a typical phenomenon for fluid stowed in aircraft tanks. The recent studies of Saltari et al. [1] showed that this type of sloshing yields substantial increase of the overall structural damping, hence its accurate prediction could make it possible to design less conservative aircraft configurations, thus enabling lighter structures.

Whereas lateral and rotational sloshing have been popular research topics for scientists and engineers [2], the literature concerning vertical motion is comparatively scarcer, probably because much less amenable to analytical treatment. Some insight can however be gained from experiments and numerical simulations [1,2,3,4] and with nonlinear reduced-order model [5, 6,7,8].

Numerical studies were initially based on potential flow models, which however require ad-hoc corrections to correctly predict energy dissipation caused by viscous effects [9]. Navier-Stokes simulations have only become available in recent times [10]. Canonical models for interface tracking based on the Volume-Of-Fluid (VOF) [11] or the Level-Set method [12] are computationally quite expensive, hence, sloshing usually has been studied with either the Particle Finite Element Method [13] and the Material Point Method [14]. A powerful alternative resides in the Smoothed Particle Hydrodynamics (SPH) approach [4,15], which is a fully Lagrangian method particularly suitable for solving fluid problems in the presence of large deformation of the free surface. However, it has been reported that in phenomena such as high fragmentation and violent free surface impacts, the predictive power of SPH is significantly reduced [16].

In this study, a high-fidelity Navier-Stokes solver based on the VOF method is used to examine liquid sloshing inside a rectangular tank set into vertical harmonic motion, with particular focus on the sloshing-induced dissipation. The equations are solved by using an energy-preserving numerical algorithm, without resorting to any turbulence model. The main reference is the recent

Materials Research Proceedings 33 (2023) 269-276 https://doi.org/10.21741/9781644902677-39

comprehensive experimental study of Saltari et al. [1], covering a wide range of excitation frequencies and acceleration amplitudes. Numerical simulations are used to get additional insight into the sloshing dynamics, especially in terms of three-dimensional effects and water/air mixing efficiency. In the experimental works mentioned above, the main attention is generally given to the flow dynamics and the resulting energy exchange between fluid and structure, but the mixing process is hardly discussed. The color function in the VOF method is here exploited to analyze the volume fractions of the two fluids across the tank, and to quantify the overall mixing efficiency. In addition, the color function allows to precisely track the position of the fluids interface, thus allowing detailed flow visualizations of the three-dimensional sloshing dynamics, even in highly chaotic configurations.

Numerical formulation

The two-phase flow of air and water taking place during the sloshing event is numerically simulated using an incompressible gas/liquid Navier-Stokes solver. The fluids are assumed to be immiscible, and the interface is implicitly tracked by means of an indicator function. The relevant governing equations are as follows

$$\nabla \cdot \mathbf{u} = 0\,, \tag{1}$$

$$\frac{\partial \boldsymbol{u}}{\partial t} + \nabla \cdot (\boldsymbol{uu}) = \frac{1}{\rho}[-\nabla p + \nabla \cdot \boldsymbol{\Sigma} + \mathbf{f_\sigma}] + \big(-\mathrm{g} + \mathrm{a(t)}\big)\mathbf{k}\,, \tag{2}$$

where $\mathbf{u} = \mathbf{u}\,(\mathbf{x}, t)$ is the fluid velocity, $p = p\,(\mathbf{x}, t)$ is the pressure, $\rho = \rho\,(\mathbf{x}, t)$ is the density, $\boldsymbol{\Sigma} = 2\mu\boldsymbol{S}$ is the viscous stress tensor, where $\mu = \mu\,(\mathbf{x}, t)$ is the dynamic viscosity and $\boldsymbol{S} = (\nabla \boldsymbol{u} + \nabla \boldsymbol{u}^T)$ is the rate of strain or deformation tensor, $a(t)$ is the acceleration imposed to the tank, g is the gravity acceleration and $\mathbf{k}$ is the unit vector oriented upwards. Although surface tension only acts at the interface, its effects are modelled as a distributed volumetric force $\mathbf{f_\sigma} = \mathbf{f_\sigma}(\mathbf{x}, \mathrm{t})$, with:

$$\mathbf{f}_\sigma = \sigma\kappa\delta(\boldsymbol{x} - \boldsymbol{x_s})\boldsymbol{n}\,, \tag{3}$$

where σ is the surface tension coefficient, κ is the local curvature of the interface between the two fluids, $\mathbf{n}$ is the unit normal to the interface, and δ is the Dirac function concentrated at the interface points $\boldsymbol{x_s}$ [17]. The Navier-Stokes equations are solved with a classical projection method [18]. Time integration is carried out by means of the Adams-Bashforth explicit scheme for the convective terms and for the off-diagonal part of the viscous terms, and the Crank-Nicolson scheme for the diagonal diffusion terms. The advection of the material interface is carried out by means of an algebraic VOF method. The numerical scheme for the advection is based on a total variation diminishing (TVD) discretization with flux limiter tailored for effective representation of binary functions [19].

Let χ be a passive tracer advected by a continuous divergence-free velocity field $\mathbf{u}$, it shall satisfy the scalar advection equation

$$\frac{\partial \chi}{\partial \mathrm{t}} + \nabla \cdot (\chi \mathbf{u}) = 0\,, \tag{4}$$

For the case of two immiscible fluids under scrutiny χ is in principle either 1 or 0. In the VOF method a color function C is introduced to approximate the cell average of χ, which in the illustrative case of one space dimension is defined as

$$\mathrm{C_i} = \frac{1}{\Delta \mathrm{x_i}} \int_{\mathrm{x_{i-1/2}}}^{\mathrm{x_{i+1/2}}} \chi(\mathrm{x}, \mathrm{t^n})\mathrm{dx}\,, \tag{5}$$

Materials Research Proceedings 33 (2023) 269-276 https://doi.org/10.21741/9781644902677-39

where $\Delta x_i = x_{i+1/2} - x_{i-1/2}$ is the cell size, while t^n is the n-th discrete time step. Equation (4) is then discretized in time yielding

$$C_i^{n+\frac{1}{2}} = C_i^{n-\frac{1}{2}} - \frac{1}{\Delta x_i}\left(\hat{f}_{i+\frac{1}{2}} - \hat{f}_{i-\frac{1}{2}}\right), \quad (6)$$

where the numerical flux $\hat{f}_{i+1/2}$ is an approximation for χ transported through the cell interface $x_{i+1/2}$ during the time interval ($t^{n-1/2}$, $t^{n+1/2}$). Details of the algorithm are provided in the original reference [20]. After computing the color function C, density and viscosity are determined by $\rho = \tilde{C}\rho_1 + (1-\tilde{C})\rho_2$ and $\mu = \tilde{C}\mu_1 + (1-\tilde{C})\mu_2$, where $\tilde{C}$ is a smoothed version of the color function, evaluated by averaging C over twenty-seven neighboring cells [20], the subscript 1 is used to denote water properties, while the subscript 2 is used for air.

The momentum equations are discretized in the finite difference framework with a staggered grid layout, where the pressure, the color function and the material properties are defined at the cell centers, whereas the velocity components are stored at the middle of the cell faces [21]. A centered second-order discretization is used for the convective terms [18,21] and diffusive terms [17], which is generally best suitable for fully resolved flows, yielding discrete preservation of the total kinetic energy in the case of uniform density. The Poisson equation is discretized by a finite-difference scheme and the resulting sparse linear system is solved by iterative methods. In particular, the HYPRE library [22] is found to be very efficient in massively parallel computations. The surface tension effects are modelled through the continuum surface force method [23], which is used to determine the equivalent local body force, and the interface curvature is evaluated through a modified version of the height function technique [20,24,25]. All details regarding the VOF solver can be found in [26].

Results and discussion

Hereafter we report the results of numerical simulations of vertical sloshing of water in air for a partially filled rectangular tank subjected to vertical sinusoidal excitation (see Fig. 1). We have carried out many two-dimensional simulations to characterize the effects of acceleration and excitation frequency on the sloshing dynamics. A tank with size $L \times H = 0.1172m \times 0.0272m$ is considered, replicating the experimental setup of Saltari et al. [1], and covered with a uniform Cartesian mesh of 128×64 grid nodes. A limited number of three-dimensional simulations has also been conducted at selected conditions to verify possible limitations of two-dimensional simulations. The governing equations are solved in a non-inertial reference frame attached to the tank, with the origin placed at the middle of its base. External excitation is modeled through imposed harmonic acceleration added to the right-hand side of the momentum equation (2), $a(t) = a_0 sin(\omega t)$, with $\omega = 2\pi f$. The initial filling level $\alpha = h/H$, expressing the quiescent fluid level as a fraction of the total depth of the tank, is set to $\alpha = 1/2$. The densities of water and air were set to $998\ Kg/m^3$ and $1.225\ Kg/m^3$, respectively, and their dynamic viscosities to $8.899 \times 10^{-2}\ Kg/(ms)$, $1.831 \times 10^{-3}\ Kg/(ms)$, respectively. The surface tension coefficient was set to 0.07199N/m.

Materials Research Proceedings 33 (2023) 269-276 https://doi.org/10.21741/9781644902677-39

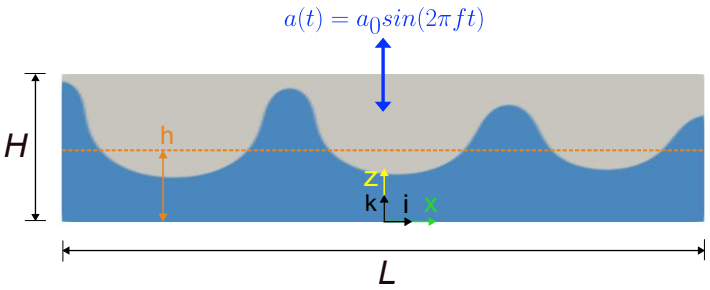

Figure 1: Computational setup for numerical simulations of vertical sloshing. L and H are the width and height of the computational domain, respectively, h is the initial level of the liquid, $a(t)$ is the vertical acceleration in vertical sloshing, f is the forcing frequency.

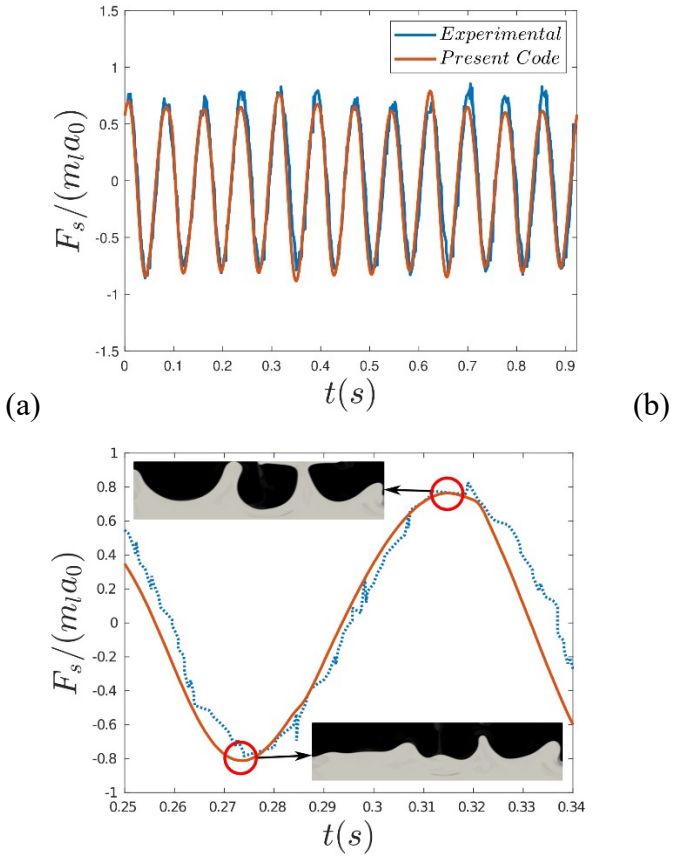

Figure 2: Time history of vertical sloshing force, compared with measurements of Saltari et al. [1] for $a_0 = 1.5g$ and $f = 13\ Hz$ (a) and detail of the sloshing force trend (b). The orange line and the blue line denote the numerical and experimental results, respectively. Instantaneous snapshots from the numerical simulation are shown at the time instants at which the sloshing force is minimum/maximum.

The sloshing vertical force is determined as

$$F_s = -\int_{walls} p\,\boldsymbol{n}\cdot\boldsymbol{k}\ dx, \tag{7}$$

Materials Research Proceedings 33 (2023) 269-276 https://doi.org/10.21741/9781644902677-39

where integration is carried out over the top and bottom walls of the tank, p is the pressure applied to the walls, and $\boldsymbol{n}$ and $\mathbf{k}$ are the wall-normal and vertical unit vector, respectively. F_s is normalized with respect to the maximum of the inertial force of the liquid, namely $m_l a_0$, with m_l the fluid mass. A quantitative comparison with the experiment carried out by Saltari et al. [1] is reported in Fig.2a, where the time history of the sloshing force over twelve forcing cycles is shown for $a_0 = 1.5g$ and $f = 13\,Hz$. We can see that the phase of the sloshing force is correctly predicted and very good agreement between simulations and experiments is found. In Fig.2b, a detail of the sloshing force in the time interval $0.25s - 0.34\,s$ is considered. Snapshots of numerical simulation illustrate the flow configuration at time instants at which the sloshing force has a (positive or negative) peak. The figure well highlights that positive peaks of the sloshing force are related to fluid impacting the ceiling of the tank, whereas negative peaks occur when the fluid retreats towards the bottom wall. This explains that a large fraction of the energy transfer between structure and fluid occurs during impacts, and that the primary mechanism for dissipation is directly associated with these fluid-structure collisions and interface fragmentation [27].

Once the vertical forces are calculated, the average work exchanged between fluid and shaker can be evaluated at any instant time t_n and over an arbitrary number $(2P)$ of periods T as

$$W(\omega, a_0) = \frac{1}{2P}\int_{t_n-PT}^{t_n+PT} F_s(\omega, a_0)\dot{s}(\tau)\ d\tau\,, \tag{8}$$

which can be expressed in nondimensional form as $\overline{W} = W/(m_l s_0^2 \omega^2)$, with s_0 displacement amplitude. The average work evaluated from numerical simulations for $a_0 = 1.5g$ and $a_0 = 3g$ is reported in Fig.3 as a function of the forcing frequency $f(Hz)$. The figure shows that for $a_0 = 1.5g$ and high forcing frequency, two-dimensional numerical simulations replicate the experimental behavior very well, whereas at $a_0 = 3g$ and/or low forcing frequency the energy dissipation is largely underestimated. These findings suggest that 2D simulations may not be appropriate to accurately characterize the energy exchanges under high forcing acceleration, where the dynamics of the air/water interface is more chaotic and three-dimensional. The numerical results obtained from 3D simulations in fact generally show improved prediction as compared to the 2D simulations. In this respect, we note that the predicted energy dissipation approaches the experimental value as the grid resolution is improved, although convergence is clearly far from being achieved, for both acceleration amplitudes. In order to accurately reproduce the fluid impacts responsible for the exchange of energy, a much finer mesh is required especially for the case with $a_0 = 3g$, where discrepancies with experimental data are more significant.

Finally, the air/water mixing process in vertical sloshing is quantified by considering the vertical profiles of the time-averaged color function, $\bar{C}(z)$. As previously pointed out, C indicates the volumetric fraction of liquid inside a computational cell, so that C = 1 means that the cell is filled with water, whereas if C = 0 the cell is filled with air. $\bar{C}$ is defined as

$$\bar{C}(z) = \frac{1}{2\Delta T}\int_{t_k-\Delta T}^{t_k+\Delta T}\left(\frac{1}{L}\int_{-L/2}^{L/2} C(x,z,t)dx\right)\ dt\,, \tag{9}$$

where the averaging interval ΔT is taken to be twenty-four forcing cycles. A global index is then introduced to quantify the overall mixing efficiency,

$$\eta = 1 - 2\sqrt{\frac{1}{H}\int_0^H (\bar{C}(z) - 0.5)^2\ dz}\,, \tag{10}$$

Materials Research Proceedings 33 (2023) 269-276 https://doi.org/10.21741/9781644902677-39

such that $\eta = 1$ in the case of perfect mixing of water and air ($\bar{C} = 0.5$), whereas $\eta = 0$ if water and air were completely segregated. Figure 4 shows the profile of η as a function of frequency for cases with $a_0 = 1.5g$ and $a_0 = 3g$. The figure shows that increasing the forcing frequency and reducing the acceleration results in less efficient mixing between fluid and air. A relatively large jump occurs between $f = 11\,Hz$ and $f = 13\,Hz$, for $a_0 = 1.5g$, which indicates the transition to the standing waves regime, implying a significant reduction of the mixing efficiency. It should also be noted that the three-dimensional simulations are in good agreement with the corresponding two-dimensional results for $a_0 = 1.5g$, whereas for $a_0 = 3g$, the 3D simulations suggest higher mixing. Higher mixing efficiency is found in cases with higher energy dissipation, i.e. lower frequency and higher acceleration. Such behavior confirms that energy dissipation is associated with fluid-structure impacts and fragmentation of the liquid-gas interface [27].

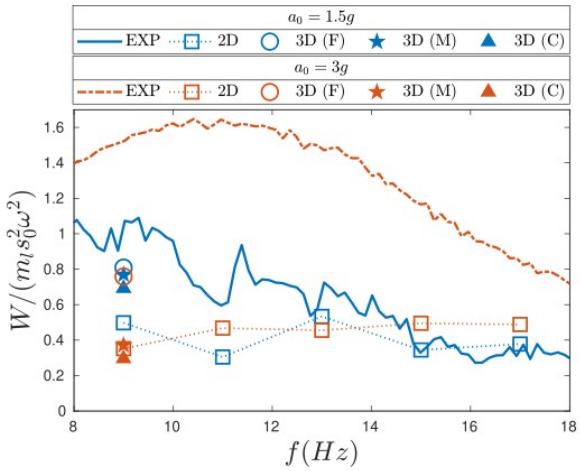

Figure 3: normalized dissipated energy $W/(m_l s_0^2 \omega^2)$ as a function of forcing frequency $f(Hz)$ for $a_0 = 1.5g$ and $a_0 = 3g$. The numerical results obtained from 2D and 3D simulations are compared with the experimental data (EXP) of Saltari et al. [1]. 3D simulations are performed with the three different grids: grid $F = 256 \times 128 \times 192$, grid $M = 192 \times 96 \times 128$, grid $C = 128 \times 64 \times 96$.

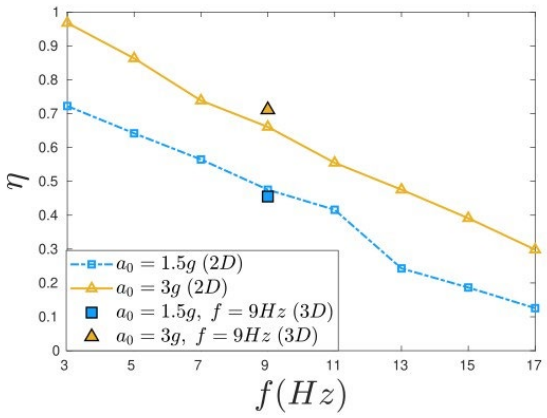

Figure 4: Mixing parameter η as a function of frequency, for $a_0 = 1.5g$ and $a_0 = 3g$.

Conclusion

By analyzing the trend of the vertical sloshing force, together with instantaneous snapshots from the numerical simulations, we concluded that positive and negative peaks of $F_s(t)$ correspond to strong liquid impacts at the top and bottom walls, which occur slightly after the inversion of the

tank motion. The characteristic flow dynamics are found to be significantly affected by the forcing parameters and to exhibit more chaotic and three-dimensional behavior in the case of strong accelerations and low forcing frequencies. Therefore, certain characteristics of the flow could not be properly reproduced by resorting only to two-dimensional simulations, and more expensive three-dimensional simulations have been carried out for comparison for the forcing frequency $f = 9\ Hz$. The results show significant improvement with respect to the 2D simulations, although the energy dissipation still exhibits some scatter. Finally, the dependence of liquid-air mixing on acceleration and frequency was quantified in terms of a global mixing efficiency indicator, arriving at the conclusion that mixing can be optimized by enhancing the acceleration amplitude and by reducing the excitation frequency. The numerical results have also highlighted that the increase of mixing corresponds to increase of the energy dissipation, suggesting that power exchanges between fluid and tank walls are closely related with the breaking of the liquid-gas interface and with fluid-wall impacts, which occur as a result of harmonic excitation. Follow-up studies might include deeper assessment of the mechanisms responsible for energy loss (e.g. impacts of liquid on the tank walls or enhanced mixing between the two phases), and assessment of the effect of turbulence models, here intentionally disregarded.

References

[1] Saltari, F., Pizzoli, M., Coppotelli, G., Gambioli, F., Cooper, J.E., Mastroddi, F., 2022a. Experimental characterisation of sloshing tank dissipative behaviour in vertical harmonic excitation. J. Fluids Struct. 109, 103478. https://doi.org/10.1016/j.jfluidstructs.2021.103478

[2] Faltinsen, O., 2017. Sloshing. Adv. Mech. .

[3] Titurus, B., Cooper, J.E., Saltari, F., Mastroddi, F., Gambioli, F., 2019. Analysis of a sloshing beam experiment, in: Proceedings of the International Forum on Aeroelasticity and Structural Dynamics, Savannah, GA, USA, pp. 10–13

[4] Calderon-Sanchez, J., Martinez-Carrascal, J., Gonzalez-Gutierrez, L.M., Colagrossi, A., 2021. A global analysis of a coupled violent vertical sloshing problem using an sph methodology. Eng. Appl. Comput. Fluid Mech. 15, 865–888. https://doi.org/10.1080/19942060.2021.1921849

[5] De Courcy, J.J., Constantin, L., Titurus, B., Rendall, T., Cooper, J.E., 2021. Gust loads alleviation using sloshing fuel, in: AIAA Scitech 2021 Forum, p. 1152. https://doi.org/10.2514/6.2021-1152

[6] Pizzoli, M., Saltari, F., Mastroddi, F., Martinez-Carrascal, J., González-Gutiérrez, L.M., 2022b. Nonlinear reduced-order model for vertical sloshing by employing neural networks. Nonlinear Dyn. 107, 1469– 1478. https://doi.org/10.1007/s11071-021-06668-w

[7] Saltari, F., Pizzoli, M., Gambioli, F., Jetzschmann, C., Mastroddi, F., 2022b. Sloshing reduced-order model based on neural networks for aeroelastic analyses. Aerosp. Sci. Technol. 127, 107708. https://doi.org/10.1016/j.ast.2022.107708

[8] Pizzoli, M., Saltari, F., Coppotelli, G., Mastroddi, F., 2022a. Experimental validation of neural-network-based nonlinear reduced-order model for vertical sloshing, in: AIAA Scitech 2022 Forum, p. 1186. https://doi.org/10.2514/6.2022-1186

[9] Antuono, M., Bouscasse, B., Colagrossi, A., Lugni, C., 2012. Two-dimensional modal method for shallow-water sloshing in rectangular basins. J. Fluid Mech. 700, 419–440. https://doi.org/10.1017/jfm.2012.140

[10] Demirbilek, Z., 1983. Energy dissipation in sloshing waves in a rolling rectangular tank — iii. results and applications. Ocean Eng. 10, 375– 382. https://doi.org/10.1016/0029-8018(83)90006-9

[11] Hirt, C.W., Nichols, B.D., 1981. Volume of fluid (VOF) method for the dynamics of free boundaries. J. Comput. Phys. 39, 201–225. https://doi.org/10.1016/0021-9991(81)90145-5
[12] Sussman, M., Fatemi, E., Smereka, P., Osher, S., 1998. An improved level set method for incompressible two-phase flows. Comput. Fluids 27, 663– 680. https://doi.org/10.1016/S0045-7930(97)00053-4
[13] Gimenez, J.M., González, L.M., 2015. An extended validation of the last generation of particle finite element method for free surface flows. J. Comput. Phys. 284, 186–205. https://doi.org/10.1016/j.jcp.2014.12.025
[14] Li, J., Hamamoto, Y., Liu, Y., Zhang, X., 2014. Sloshing impact simulation with material point method and its experimental validations. Comput. Fluids 103, 86–99. https://doi.org/10.1016/j.compfluid.2014.07.025
[15] Colagrossi, A., Landrini, M., 2003. Numerical simulation of interfacial flows by smoothed particle hydrodynamics. J. Comput. Phys. 191, 448– 475. https://doi.org/10.1016/S0021-9991(03)00324-3
[16] Banim, R., Lamb, R., Bergeon, M., 2006. Smoothed particle hydrodynamics simulation of fuel tank sloshing. Proceedings 25th international congress of the aeronautical sciences .
[17] Tryggvason, G., Scardovelli, R., Zaleski, S., 2011. Direct Numerical Simulations of Gas-Liquid Multiphase Flows. Cambridge University Press.
[18] Orlandi, P., 2012. Fluid flow phenomena: a numerical toolkit. volume 55. Springer Science & Business Media.
[19] Pirozzoli, S., Di Giorgio, S., Iafrati, A., 2019. On algebraic TVD-VOF methods for tracking material interfaces. Comput. Fluids 189, 73–81. https://doi.org/10.1016/j.compfluid.2019.05.013
[20] Popinet, S., 2009. An accurate adaptive solver for surface-tension-driven interfacial flows. J. Comput. Phys. 228, 5838–5866. https://doi.org/10.1016/j.jcp.2009.04.042
[21] Harlow, F.H., Welch, J.E., 1965. Numerical calculation of time-dependent viscous incompressible flow of fluid with free surface. Phys. Fluids 8, 2182–2189. https://doi.org/10.1063/1.1761178
[22] Falgout, R.D., Yang, U.M., 2002. hypre: A Library of High Performance Preconditioners, in: International Conference on computational science, pp. 632–641. https://doi.org/10.1007/3-540-47789-6_66
[23] Brackbill, J.U., Kothe, D.B., Zemach, C., 1992. A continuum method for modeling surface tension. J. Comput. Phys. 100, 335–354. https://doi.org/10.1016/0021-9991(92)90240-Y
[24] Cummins, S.J., Francois, M.M., Kothe, D.B., 2005. Estimating curvature from volume fractions. Comput. Struct. 83, 425–434. https://doi.org/10.1016/j.compstruc.2004.08.017
[25] Francois, M.M., Cummins, S.J., Dendy, E.D., Kothe, D.B., Sicilian, J.M., Williams, M.W., 2006. A balanced-force algorithm for continuous and sharp interfacial surface tension models within a volume tracking framework. J. Comput. Phys. 213, 141–173. https://doi.org/10.1016/j.jcp.2005.08.004
[26] Di Giorgio, S., Pirozzoli, S., Iafrati, A., 2022. On coherent vortical structures in wave breaking. J. Fluid Mech. 947, A44. https://doi.org/10.1017/jfm.2022.674
[27] Marrone, S., Colagrossi, A., Di Mascio, A., Le Touzé, D., 2015. Prediction of energy losses in water impacts using incompressible and weakly compressible models. J. Fluids Struct. 54, 802–822. https://doi.org/10.1016/j.jfluidstructs.2015.01.014
/